Applied Catalysis B: Environmental 100 (2010) 413–426

Contents lists available at ScienceDirect

Applied Catalysis B: Environmental

journal homepage: www.elsevier.com/locate/apcatb

Review

Composite materials: An emerging class of fuel cell catalyst supports

Ermete Antolini[a,b,*]

[a] Scuola di Scienza dei Materiali, Via 25 aprile 22, 16016 Cogoleto, Genova, Italy
[b] Instituto de Química de São Carlos, USP, C. P. 780, São Carlos, SP 13560-970, Brazil

ARTICLE INFO

Article history:
Received 7 May 2010
Received in revised form 20 August 2010
Accepted 27 August 2010
Available online 29 September 2010

Keywords:
Fuel cells
Catalyst supports
Platinum
Hybrid materials

ABSTRACT

Highly dispersed platinum or platinum-based catalysts on a conductive support are commonly used as electrode materials in low-temperature fuel cells. The performance and, in particular, the stability of these catalysts strongly depend on the characteristics of the support. Being the use of plain carbon, ceramic or polymer materials not completely satisfactory, in the last years hybrid polymer–carbon, ceramic–carbon and polymer–ceramic materials have been proposed as fuel cell catalyst supports. These hybrid materials, possessing the properties of each component, or even with a synergistic effect, would present improved characteristics with respect to the bare components.

In this paper we present an overview of these hybrid materials as low-temperature fuel cell catalyst supports. The improved characteristics of the mixed supports with respect to the individual component and their effect on the electrochemical activity are highlighted.

Contents

1. Introduction

Low-temperature fuel cells represent environmentally friendly technologies and are attracting considerable interest as a means of producing electricity by direct electrochemical oxidation of hydrogen or low-molecular-weight alcohols [1–3]. Highly dispersed platinum or platinum-based catalysts on a conductive support are commonly used as electrode materials for oxidation and reduction reactions [4]. In such catalysts, the high surface to volume ratio of metal particles maximizes the area of the surface available for the reactions. The structure and proper dispersal of these metal particles make low-loading catalysts feasible for fuel cell operation, lowering the cost of the system. The main requirements of a suitable fuel cell catalyst support are (i) high surface area, to obtain high metal dispersion, (ii) suitable porosity, to boost gas flow, (iii)

* Corresponding author at: Instituto de Química de São Carlos, USP, C. P. 780, São Carlos, SP 13560-970, Brazil. Tel.: +55 33739899; fax: +55 33739895.
E-mail address: ermantol@libero.it.

0926-3373/$ – see front matter © 2010 Elsevier B.V. All rights reserved.
doi:10.1016/j.apcatb.2010.08.025

high electrical conductivity, and (iv) high stability under fuel cell operational conditions.

At present, carbon, in particular Vulcan XC-72 carbon blacks, is the common choice for supporting nanosized electrocatalyst particles in low-temperature fuel cells because of its large surface area and high electrical conductivity [5]. A major problem regarding the use of carbon blacks as fuel cell catalyst support, particularly as cathode catalyst support, is their low resistance to corrosion caused by electrochemical oxidation of the carbon surface. As reported by Couper et al. [6], the problems of finding a good electrocatalyst for the oxygen reduction reaction (ORR) and a stable, inert substrate are compounded by the instability of most materials to corrosion close to the reversible potential for the O_2/H_2O couple. The instability of carbon support affects the loss of platinum surface area following both platinum particle sintering and platinum release from the carbon support [7–9]. Notwithstanding the acid environment is less severe and operation temperature is lower in polymer electrolyte fuel cells (PEMFCs) than in PAFCs, corrosion of the cathode catalyst support also affect the durability of the PEMFCs [10–12]. On the other hand, the anode catalyst could also be exposed to much more oxidative conditions than the cathode during the cell voltage reversal caused by fuel starvation [13]. Summarizing, high-surface-area carbon supports in PAFC and PEMFC electrodes are susceptible to corrosive conditions, which include high water content, low pH, high temperature, high potential, and high oxygen concentration. In addition, Pt catalysts seem to accelerate the rate of carbon corrosion [14]. Moreover, carbon blacks have high specific surface area, but contribute mostly with micropores of less than 1 nm. The presence of micropores is a disadvantage when the carbon is used as catalyst support. Indeed, when the average diameter of the pores is less than 2 nm, the supply of the fuel to the surface may not occur smoothly and the activity of the catalyst may be limited [5]. In the same way, the presence of a high amount of micropores results in a low accessible surface area for the deposition of metal particles. Finally, carbon does not conduct protons, which limits the achievable performances. In order to facilitate transport of protons within the catalyst layer and thereby obtain maximum utilization of the catalyst, a proton-conducting polymer (*e.g.*, Nafion®) is usually mixed with the catalyst.

Therefore, various alternatives of electrocatalyst supports are being searched. Due their high surface area and high amount of mesopores, which allow high metal dispersion and good reactant flux, ordered mesoporous carbons and carbon gels have been receiving attention as fuel cell catalyst supports. Catalysts supported on these carbons showed higher catalytic activity than the same catalysts supported on carbon black. Their stability in fuel cell environment, however, is almost the same to that of carbon blacks [5]. Recently, nanostructured carbon materials with graphitic structure, such as carbon nanotubes (CNTs) and carbon nanofibers (CNFs) were investigated as catalyst supports in fuel cells [5]. The higher catalytic activity of Pt and bimetallic Pt-based catalysts supported on CNT and CNF than that of the same catalysts supported on carbon blacks was ascribed to their unique structure and properties such as high surface area, good electronic conductivity and chemical stability [5]. Tests carried out in PEM fuel cell conditions indicated that these materials can be more durable and can outlast the lifetime of conventional Vulcan XC-72 carbon black [15–17]. However, these alternative materials do not prevent carbon oxidation, but rather simply decrease the rate. Moreover, CNTs normally possess outer diameter of 10–50 nm, inside diameter of 3–15 nm (pore size), and a tube length of 10–50 μm. During synthesis of the catalyst using this support, Pt particles (2–5 nm size) present on the pore mouths of CNTs will take part in the chemical reaction. However, there is a great possibility for the existence of Pt particles inside the nanotube, depending on Pt particle size. These particles will take little part in the chemical reaction. The number of the Pt particles inside the tube will be more when the tube length of CNT increases. So, a decrease of the Pt active area and the electrochemical activity of the catalyst have to be expected.

For this reason non-carbon materials have been investigated as catalyst supports [18,20]. Conducting oxides are emerging candidates as oxidation-resistant catalyst supports. These materials are thermally and electrochemically stable in fuel cell environment and present excellent resistance to corrosion in various electrolytic media. In addition to their high stability in the fuel cell environment, unlike carbon, which does not enhance electrocatalytic activities, but serves only as a mechanical support, many metal oxide supports can act as co-catalysts. Indeed, it is well known that metal oxides such as RuO_2, SnO_2 and WO_3 enhance the catalytic activity of platinum for methanol and ethanol oxidation [19–24]. However, a major problem of ceramic oxides is their low surface area, resulting in a low metal dispersion and, as a consequence, in a low catalytic activity of the supported metals. Moreover, the electronic conductivity of some metal oxides such as TiO_2 and SnO_2 is very low at temperatures below 200 °C.

Given their structural characteristics, conducting polymers (CPs) have been proposed as supports for low-temperature fuel cell catalysts [25]. Generally, conducting polymers fulfill the main requirements of a suitable fuel cell catalyst support: they possess high surface area, to obtain high metal dispersion, suitable porosity, to boost gas flow, high electrical conductivity, and high stability under fuel cell operational conditions. Some CPs are not only electron conducting, but also proton-conducting materials, so they can replace Nafion® in the catalyst layer of fuel cell electrode and provide enhanced performance. In this case, theoretically only a two-phase boundary is necessary for electron and ion transfer during reactions in fuel cells compared to the three-phase boundary when carbon is used. The most used CPs are conjugated polymers with heteroatoms in the main chain (heterocyclic polymers) as polyaniline (PAni), polypyrrole (PPy), polythiophene (PTh) and their derivatives. For PPy and, particularly, PAni supported catalysts, in addition to an increase of metal surface area, the enhancement of their catalytic activity was ascribed to a synergic effect between the metal and the polymer matrix [25]. Generally, CP-supported catalysts show an acceptable stability (i.e., film integrity and catalytic activity) under fuel cell conditions. However, PAni and PPy chemical degradation was observed both during metal deposition and during the catalytic processes. The electronic conductivity of the polypyrrole was seriously degraded by the deposition of the catalyst particles under both reducing and oxidizing conditions [26]. Polyaniline degradation by aldehydes, intermediate products of methanol and ethanol oxidation, was also observed [27]. The supported catalyst can promote polymer degradation [28]. Moreover, the loss of electronic conductivity of polypyrrole and polyaniline in the potential range for oxygen reduction is a major limitation for their use as electrocatalyst supports.

Summarizing, the use of either carbon or ceramic or polymer materials as fuel cell catalyst support is not completely satisfactory. Thus, in the last years composite polymer–carbon, ceramic–carbon and polymer–ceramic materials have been proposed as fuel cell catalyst supports. These composite materials can possess more suitable properties for their use as catalyst supports than their individual components. For example, the combination of PAni with CNTs would offer an attractive composite support material for electrocatalyst to enhance its activity and stability based on morphological modification and/or electronic interaction between two components [29]. Regarding the polymer-containing composites, Gomez-Romero [30] classified them into two major groups, according to the nature of the host and guest phases. Thus, organic–inorganic (OI) materials will denote hybrids where the organic phase is host to an inorganic guest, whereas

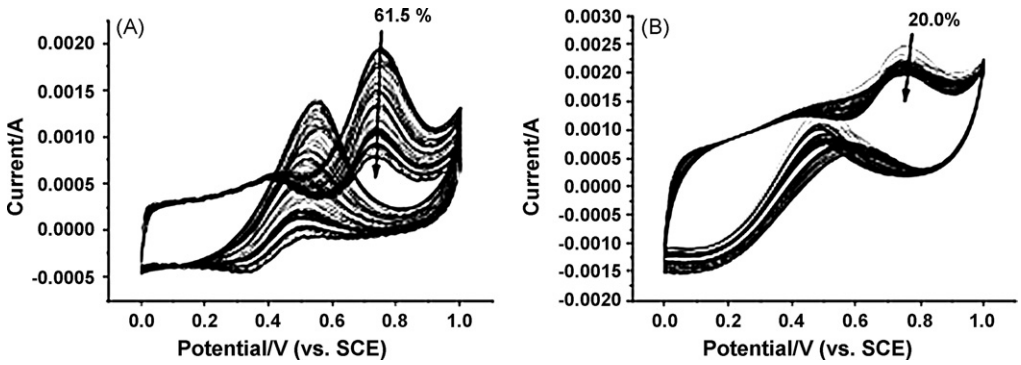

Fig. 1. CV curves for platinized-carrier-modified electrodes in 1.0 M H_2SO_4 + 1.0 M CH_3OH medium. (A) Pt/C, for 200 cycles; (B) Pt/0.25:1 PAni–C, for 200 cycles. Reproduced from Ref. [32], copyright 2007, with permission from Elsevier.

inorganic–organic (IO) materials will be those with inorganic hosts and organic guests. Obviously there will be cases falling right at the frontier between these two major classes. In addition to the above-mentioned classification, the inorganic species which will form the hybrid materials can be either molecular or extended in nature. This will have obvious implications in the nature of the hybrid compounds, a field in which the 10 Å molecular dimension, the 10^2 Å polymer chain dimension, and the 10^3 Å crystal grain dimension will need to be considered together. In OI hybrids, the inorganic molecules will in general contribute their chemical activity and will need the structural support of CPs to become part of useful solid materials. In IO hybrids on the other hand, it will be the inorganic phase fulfilling the structural task although the inserted CPs can also imprint their polymeric nature onto the materials obtained. In between the two major groups of hybrids we will find nanocomposite materials where none of the phases dominates the structure.

In this paper, an overview of some composite polymer–carbon, ceramic–carbon and polymer–ceramic materials proposed as low-temperature fuel cell catalyst supports, is presented. The improved characteristics of the mixed supports with respect to the individual component and their effect on the electrochemical activity are highlighted.

2. Composite polymer–carbon supports

2.1. General overview

Firstly, it has to be distinguished into three types of polymer–carbon supported catalysts: (1) catalysts supported on effective hybrid polymer–carbon materials, (2) dendrimer-encapsulated catalysts supported on carbon substrates, and (3) catalysts supported on ionomer-coated carbon powders. Only the hybrid polymer–carbon materials can be considered as novel supports with properties other than the single components. Dendrimers are used for preparing metal nanoparticles because they can act as structurally and well-defined templates and robust stabilizers. Dendrimer template and terminal amine functional groups provide for uniform preparation of size-monodisperse catalysts and facilitates the controlled dispersion and loading of the catalysts onto carbon supports. Finally, incorporation of ionomer (commonly Nafion®) in the carbon support enhances the contact area between the catalyst particles and ionomer and reduces the total amount of ionomer required in the anode catalyst layer. The substantial difference between hybrid polymer–carbon, dendrimer–carbon and ionomer–carbon composites is the following: only the first composite is formed by two components which both can act as a catalyst support, whereas the in last two composites only the carbon can acts as a plain support for fuel cell catalysts.

2.2. Hybrid polymer–carbon supports

The preparation of porous hybrid organic–inorganic nanomaterials has generated a great deal of interest since they exhibit properties that cannot be attained by their individual components [30]. As an example, the formation of nanocomposites with inorganic materials and conducting polymers has been found to enhance the thermal, mechanical, electrical and chemical properties of the latter [31]. The polymer in these materials is commonly synthesized *in situ*, either inside the pores of an inorganic host or coating the surface of inorganic guest. Among various inorganic materials, porous carbons are especially attractive because of their availability in a wide variety of physical structures, large internal surface areas, and porosities. In the following part of Section 2.2 the use of conducting polymers mixed with carbon blacks or carbon nanotubes as fuel cell catalyst supports is presented

2.2.1. Hybrid polymer–carbon blacks supports

Generally the electrochemical activity of catalysts supported on mixed polymer–carbon blacks, commonly Vulcan XC-72, is higher than that of the same catalysts supported on the single carbon [32–34] or the single polymer [35]. This improvement has been ascribed to the higher available surface area and electronic conductivity of the support and easier charge-transfer at the polymer/electrolyte interface allowing a high utilization of deposited metal nanoparticles. Xu et al. [32] and Wu et al. [35] prepared PAni–C composites by chemical and electrochemical polymerization of aniline in the presence of carbon, respectively. The effect of carbon presence on the resulting PAni characteristics was different: while in the former case the presence of carbon does not affect the chain structure of PAni, a higher polymeric degree and a lower defect density in the PAni structure was observed for the electrochemically polymerized PAni in the presence of carbon. The electropolymerization rate of aniline was undoubtedly accelerated by the incorporation of carbon particles. Xu et al. [32] mainly studied the effect of PAni presence on carbon characteristics (IO material). An optimal mass ratio of PAni to C (PAni:C = 0.25:1) was found. An excess of PAni will decrease the conductivity of the composite, whereas a too little amount of PAni will decrease the anti-poisoning ability of the catalyst. After 200 potential cycles, the decrease of methanol oxidation current by the CO poisoning intermediate products was 61.5% on the Pt/C catalyst, but only 20% on the Pt/PAni–C composite catalyst, as can be seen in Fig. 1 from Ref. [32]. The anti-poisoning ability of Pt/PAni–C was three times higher than that of Pt/C. The presence of PAni supports water absorption on the catalyst, and formation of an active oxycompound Pt–OH_{ads}, which promotes CO oxidation to CO_2. The work of Wu et al. [35], instead, was addressed to the effect of the addition of carbon particles to PAni (OI material). They observed that the incorporation

of carbon particles not only increases the electron conductivity of the PAni film, but also decreases charge-transfer resistance at PAni/electrolyte interfaces. In both case, the platinum dispersion on PAni–C and the activity for methanol oxidation of supported Pt was considerably higher than that of the single host component, Pt/C [32] and Pt/PAni [35], respectively. Unlikely from the previous works, Gharibi et al. [33] prepared a hybrid PAni–C support by mixing carbon Vulcan XC-72 and presynthesized PAni doped with trifluoromethane sulfonic acid. Then, the PAni–C composite was impregnated with H_2PtCl_6, followed by Pt reduction with $NaBH_4$. The electrochemically active area (EAS), the activity for methanol oxidation and the stability of Pt/PAni–C was higher than that of a commercial Pt/C by E-Tek. They observed that PAni provides improvements in both electron and proton conductivities at the electrodes, increases the methanol diffusion coefficient at the electrode by a factor of 2, decreases the onset potential of methanol oxidation and the catalyst susceptibility to poisoning.

Zhao et al. [34,36] and Mokrane et al. [37] synthesized polypyrrole-Vulcan XC-72 carbon composites by *in situ* chemical oxidative polymerization of pyrrole monomer on carbon powders. Zhao et al. [34] prepared a novel catalyst support by polymerization of pyrrole on carbon powders with and without the presence of naphthalene sulfonic acid (NSA). Then, 40 wt% Pt/PPy–C catalysts were prepared by the chemical reduction method. Cyclic voltammetry (CV) measurements of the hydrogen and methanol oxidation reactions (HOR and MOR, respectively) showed that Pt nanoparticles deposited on PPy–C with NSA as dopant possess higher catalytic activity than those on plain carbon and on PPy–C without NSA. This result might be due to the higher accessible surface area and the higher conductivity, allowing a high utilization of deposited Pt nanoparticles. Nanostructured and mixed-conducting PPy as a component of the catalyst support is favorable for setting up an effective conducting network for electron and proton transportation and may assist platinum deposition. NSA doping in the PPy–C composite could further enhance the conducting ability of the support. In a next work, Zhao et al. [36] synthesized a Pt–Fe/PPy–C catalyst by *in situ* interfacial polymerization combined with metallic co-precipitation. This catalyst showed a high electrochemical activity for methanol oxidation, ascribed to the ultrafine and uniform metal catalyst dispersion on the surface of the support. In addition, PPy-modified carbon would improve the stereo structure of catalyst system, and some micropores of carbon might be clogged by PPy, which can prevent $PtCl_6^{2-}$ from diffusing into micropores of carbon and improve the utilization of Pt. Mokrane et al. [37] synthesized PPy–C composites with different PPy/C ratios. They observed that the nature of the composite strongly influences the electrochemical activity of supported platinum toward the oxygen reduction reaction in acid medium. The variation of the PPy/C ratio determines the so-called substrate effect for electrocatalysis. The ORR decreases with increasing PPy content in the composite. In this case the effect of the mixed support on the catalytic activity of Pt is negative, as IO material, with respect to pure carbon support, and negligible, as OI material, in comparison with pure PPy.

2.2.2. Hybrid polymer–CNT supports

Among various types of carbons, the most part of the studies on polymer–carbon composites was addressed to carbon nanotubes as carbon materials due their unique properties. To comprehend the various aspects of polymer–CNT composites, detailed understanding of the chemistry, structure and properties of CNT is crucial. Carbon nanotubes are cylindrical shells made by rolling graphene sheets. A graphene sheet consists of a monolayer of sp^2-bonded carbon atoms where each atom is connected to three carbon atoms in the *x*–*y* plane and a weak delocalized 'π-electron' cloud in the *z* axis which gives CNT its unique electrical properties [38]. There are two basic types of CNT, that is, SWNT (single wall carbon nanotubes) and MWNT (multiwall carbon nanotubes). SWNT consist of a single graphene sheet, which is a planar array of benzene molecules, involving hexagonal rings with double and single carbon–carbon bonding. MWNT comprise an array of such nanotubes that are concentrically nested. The unique properties associated with CNT depend by various factors, that is, synthesis method, degree of graphitization, defects, chirality, diameter and degree of crystallinity and entanglements [39,40]. Concerning the structure effect, it has been reported that the end-caps of nanotubes are highly reactive as compared to the sidewalls [41], which themselves contain defect sites in the nanotubes lattice. This intrinsic defect chemistry paves way to tether many different types of chemical moieties onto the defect sites which can further be utilized to tailor the polymer/CNT interface.

Generally, polymer–CNT composites are OI materials, where CNT are dissolved in the polymer matrix to improve the electrical and mechanical properties of the polymer. The properties of polymer–CNT composites depend on a multitude of factors that include the type (SWNT, MWNT), chirality, purity, defect density, and dimensions (length and diameter) of the nanotubes, nanotube loading, dispersion state and alignment of nanotubes in the polymer matrix, and the interfacial adhesion between the nanotube and the polymer matrix [39]. The possibility to achieve reasonably high conductivity at low CNT content owing to its high aspect ratio makes them an ideal candidate to be harnessed for several potential applications. Such high aspect ratio facilitates CNT to form a 'network-like' structure in the composites at a particular often low concentration termed as 'percolation'. However, in order to exploit the exceptional properties of CNT one has to design strategies to generate in a reproducible way a stable and uniform dispersion of CNT in the composites. The strong inter-tube van der Waals' forces impede the uniform dispersion of CNT and the nanotubes are often dispersed as aggregates in the matrix. In addition, certain properties of the host polymer matrix like wetting, polarity, crystallinity, melt-viscosity etc. add to the challenge of obtaining a percolative 'network-like' structure of CNT in the composites at a desired concentration. Hence the level of percolation varies vastly with the matrix polymer [42]. The biggest issues in the preparation of CNT-reinforced composites reside in efficient dispersion of CNT into a polymer matrix, the assessment of the dispersion, and the alignment and control of the CNT in the matrix. Thus, several methods have been employed for the dispersion of nanotubes in the polymer matrix such as solution mixing, melt mixing, electrospining, *in situ* polymerization and chemical functionalization of the carbon nanotubes [43].

2.2.2.1. Hybrid polyaniline-carbon nanotube (PAni–CNT) supports. PAni–CNT composites are the most investigated hybrid supports for fuel cell catalysts. Polyaniline is a conducting polymer of the semi-flexible rod polymer family. Among the family of conducting polymers, PAni is unique due to its ease of synthesis, environmental stability, and simple doping/dedoping chemistry. PAni presents a wide range of conductivity (15 orders of magnitude) including conductivity values that approach 5 S cm^{-1} [44]. The conduction mechanism of PAni includes the exchange of both electrons and protons [44]. The key developments in PAni–CNT composites have been reviewed by Gajendran and Saraswathi [45]. Almost all the properties of the composites depend on their preparation method and on CNT content. Apart from *in situ* chemical polymerization and electrochemical deposition, a number of interesting approaches including the use of aniline functionalized CNT and ultrasound/microwave/gamma-radiation initiated polymerization have been used in the preparation of composites. Importantly, the extensive possibility of functionalizing the CNT should pave way for the preparation of new PAni–CNT composites. The acid-treated CNT is suitable for providing a better interaction with PAni. The

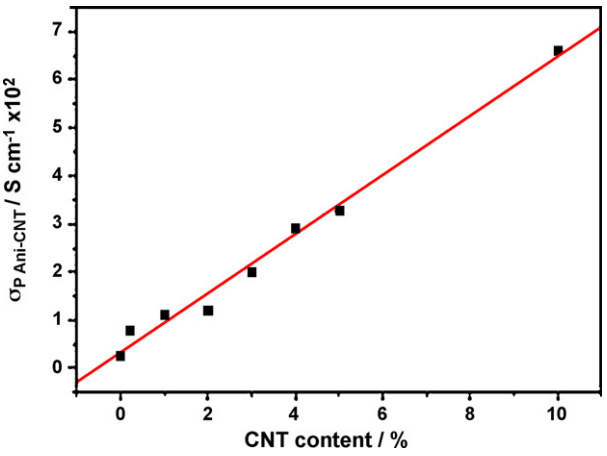

Fig. 2. Dependence of PAni–CNT electronic conductivity ($\sigma_{PAni-CNT}$) on CNT content from the data reported in Ref. [46].

integration of PAni with the acid-treated CNT in the form of a composite material has resulted in a simple procedure for dissolving the doped PAni in aqueous solutions. Indeed, an interesting characteristic of PAni–CNT composites is their easy dispersibility in aqueous solution. The structure and properties of these composites have been investigated by a variety of techniques including absorption, infrared (IR), Raman, X-ray photoelectron spectroscopy methods, scanning electron and scanning probe microscopy techniques, cyclic voltammetry, and thermogravimetry, and the experimental results indicated favorable interaction between PAni and CNT. Unlike other conducting polymers like PPy or PTh, PAni showed strong interactions with CNT, resulting in a synergetic performance of the composites in several applications [45].

PAni–MWNT composites, prepared by mixing MWNT with aniline, followed by *in situ* polymerization, showed drastic increase in electrical conductivity [46]. As shown in Fig. 2, obtained from the data reported in Ref. [48], the conductivity of the hybrid materials ($\sigma_{PAni-CNT}$) increased almost linearly with increasing of CNT content. When the CNT content increased to 10%, the conductivity of the composite was more than 25 times than that of the parent PAni. Even 0.2% of CNT can improve the conductivity of the PAni–CNT composite more than 3 times than that of PAni. The network including PAni fibers and CNT forms new conductive passageway, which account for the high conductivity. On these bases, the PAni–CNT composites can serve as excellent host matrices for fuel cell catalysts. The metal-impregnated mixed composites have been used as electrode materials for methanol, formaldehyde and formic acid oxidation [47–52]. Generally, the size of the metal nanoparticles deposited on the composite matrix is smaller than that on PAni. This gives a higher dispersion and better utilization of the metal nanoparticle-impregnated composites, resulting in their high performance and stability. Shi et al. prepared PAni–CNT composites by electropolymerization of aniline containing well-dissolved SWNT [47] or MWNT [48]. Then, platinum particles were electrodeposited on the composite films. The electrical conductivity of PAni–CNT composites was considerably higher than that of pristine Pani. The porosity of the PAni film significantly changes by the introduction of MWNT. The PAni–MWNT composite films show a considerable quantity of fibers of diameter about 100 nm together with a small quantity of spherical grains. The fibers entangled to form a relatively uniform web and made the film more highly porous. During the growth process, MWNTs are uniformly dispersed in PAni matrix and may serve as condensation nuclei. Therefore, they were coated with a considerable amount of PAni to form such a fibrous material. The higher degree of porosity than pure PAni favors the dispersion of platinum particles on the composite films. The electrocatalytic activity of Pt/PAni–SWNT and Pt/PAni–MWNT electrodes was significantly higher than that of Pt/PAni electrode toward formic acid and methanol oxidation, respectively. Wu et al. [49] and Wang et al. [50] prepared PAni–SWNT composites by electrochemical polymerization of aniline in the presence of SWNT. Then, Pt particles were electrodeposited on the PAni–SWNT films by H_2PtCl_6 reduction at constant potential. In both cases, the characteristics of PAni were affected by the presence of SWNT. Wu et al. [49] found that the rate of aniline polymerization was enhanced by the presence of SWNT. The PAni/SWNT composite film showed a higher polymeric degree and lower defect density in PAni structure than pure PAni film. Furthermore, the incorporation of SWNT also lead to higher accessible surface area, electronic conductivity and easier charge-transfer at the polymer/electrolyte interface, which make higher utilization for deposited Pt. SEM images by Wang et al. [50] showed that the pure PAni film has typical spherical grain morphology (Fig. 3a), and it coalesced, making the surface rough with no uniformity. But the morphology of PAni film significantly changed by the introduction of 0.8 wt% SWNT, which shows a considerable quantity of fibers (of diameter about 100 nm) together with some spherical grain (Fig. 3b). For the composite film, SEM images revealed the uniform and cable-like morphology of the nanostructures in which the outer layers were polyaniline and the inner layer were comprised of SWNT. As can be seen in Fig. 3b, the film displays a new interwoven fibrous structure, and the fibers are less densely packed, making the film smooth, uniform, and highly porous. Such a uniform and porous morphology is desirable because it enables a material with high ionic conductivity to achieve fast charge/discharge rates. Fig. 3c shows the SEM of Pt-modified PAni–SWNT composite film. The white spots in the micrograph can be attributed to platinum micro-particles. Pt particles are spread in a homogeneous arrangement on polymer matrix. For the porous structure and high surface of PAni–SWNT composite film, the platinum atoms are readily grown and formed small clusters what favors it to achieve a high degree of dispersion. As a consequence, Pt particles electrodeposited on the PAni–SWNT composite film showed excellent catalytic activity and stability for the electro-oxidation of methanol [49] and formaldehyde [50] in comparison to Pt supported on PAni film.

As previously reported, the insolubility and poor compatibility of CNTs with the polymer limited the feasibility of synthesizing this kind of composite. To overcome this problem, Zhu et al. [51], to prepare homogeneous PAni–MWNT nanocomposites, functionalized the MWNT via the diazotization reaction. The 4-carboxylicbenzene group was modified on a MWNT surface via a C–C covalent bond, which supports the dispersion of carbon nanotubes in aniline. Then, electrochemical polymerization was induced by cyclic voltammetry in H_2SO_4 containing aniline and 0.8 wt% MWNT. The functionalization of the MWNT can ensure the compatibility of carbon nanotubes in the polyaniline matrix, which can avoid potential microscopic phase separation in the nanocomposite. The PAni–MWNT composite films modified by electrochemically depositing platinum showed much higher mass activity and long-term stability for formic acid oxidation than a pure PAni film.

Unlikely to the abovementioned PAni–CNT composite, Santhosh et al. [52] prepared a PAni–CNT composite belonging to the IO group. They grafted PAni chains onto amine-functionalized MWNT (MWNT–NH_2) by electropolymerizing a mixture of aniline and MWNT–NH_2 using cyclic voltammetry. Then, Au nanoparticles were dispersed into the film of PAni-g-MWNT by electrochemical reduction of $HAuCl_4$. Grafting of PAni on MWNT surfaces masks the defect sites in MWNT and provides a uniform surface with positively charged (protonated amine/imine) sites. The positive charges from the aniline units in PAni electrostatically absorb gold ions, creating a sink of gold ions in the matrix. Au nanoparticle formation

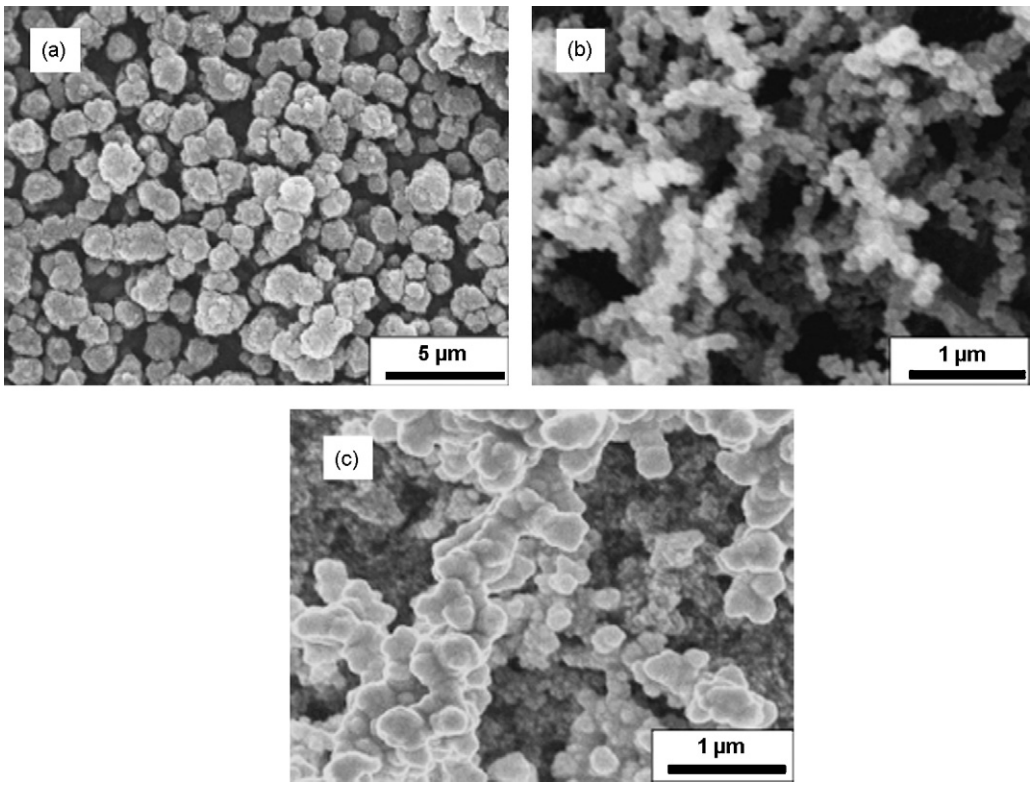

Fig. 3. Typical SEM images of the pure PAni (a), PAni–SWNT composite (b) with a content of SWNTs 0.8%, and the Pt-modified PAni–SWNT film (c). Reproduced from Ref. [50], copyright 2007, with permission from Elsevier.

is expected to occur at the adsorbed sites, hence avoiding aggregation. Field emission transmission electron microscopy (FETEM) images indicated that Au particles of 8–10 nm in size are uniformly distributed into PAni-g-MWNT. The electrocatalytic activity of the Au/PAni-g-MWNT electrode toward oxidation of methanol was higher than that of Au/MWNT and pristine An electrodes. Methanol oxidation at the Au/PAni-g-MWNT occurs at a much lower oxidation potential (780 mV) electrode and with high current densities compared with the Au/MWNT electrode (890 mV) and pristine Au electrode (930 mV). The enhanced MOR activity of the Au/PAni-g-MWNT electrode was ascribed to the lower crystallite size of Au nanoparticles and the uniform distribution of Au nanoparticles in the three-dimensional PAni-g-MWNT network. The presence of PAni as a grafted chain onto MWNT electrostatically stabilizes the Au nanoparticles and prevents aggregation of particles. As a result, smaller particles of Au can be distributed in the PAni-g-MWNT matrix.

2.2.2.2. Other hybrid polymer–CNT supports. Hybrid polymer–CNT composites with the polymer other than PAni have been tested as fuel cell catalyst supports. Selvaray et al. [53,54], Qu et al. [55] and Bae et al. [56] synthesized hybrid PPy–MWNT films by *in situ* chemical polymerization, in which the matrix material was either PAni (OI material) [53,54] or MWNT (IO material) [55,56]. Carbon nanotubes are relatively good electron acceptors, while PPy can be considered a good electron donor. The PPy may serve as "conducting bridges" among the carbon nanotubes. The average diameter of the nanotubes increases with increasing PPy content in the composite. Pt and Pt-based catalysts were then deposited on the PPy–MWNT composites by chemical reduction of the corresponding metal [53–55] or by γ-irradiation induced reduction of Pt and Ru ions [56]. In the case of PPy imbedded in the MWNT matrix, the existence of PPy layer which was evenly wrapped on the surface of MWNTs resulted in significant improvement in Pt particle dispersion and a higher Pt content on PPy–MWNT supports than that on MWNT [55,56]. Bae et al. [56] attributed the high catalyst dispersion to the change from hydrophobic surface of pristine MWNT to a more hydrophilic PPy coated-MWNT surface. These PPy–MWNT supported catalysts showed high activity for methanol, formic acid and formaldehyde oxidation. In particular the MOR activity of the Pt/PPy–MWNT catalyst was higher than that of Pt/PPy [54] and Pt/MWNT [55] catalysts.

Poly(*N*-acetylaniline) (PAANI), one of substituted polyaniline conducting polymers, was successfully used as a support for fuel cell catalysts [57]. On this basis, Jiang et al. [58] prepared a novel 3D nanorods matrix of PAANI/MWNT (in which the inner layer was comprised of MWNT and the outer layer was PAANI, forming a core-shell structure) by electropolymerization of *N*-acetylaniline in the presence of the nanotubes. Spherical Pt nanoparticles of ca. 50–500 nm distributed along the PAANI/MWNT composite film chain, forming a nanoparticles–nanorod–nanoparticles network, were obtained by Pt electrodeposition, and Pt particles inside the matrix are much smaller than the outside ones. The resulting Pt/PAANI–MWNT/GC electrode was used for the catalytic oxidation of formaldehyde in acidic solution. It was found that the Pt/PAANI–MWNT/GC electrode has enhanced electrocatalytic activity and stability toward the formaldehyde oxidation and significantly reduced poisoning effect compared to the Pt/PAANI/GC electrode. The PAANI–MWNT film presented a much lower electrochemical charge-transfer resistance than the pure PAANI film, suggesting its more active sites for faradaic reactions and easier charge-transfer at the interface owing to the presence of the incorporated MWNT. Furthermore, the electrostatic interaction between PAANI and MWNTs facilitates the effective degree of electron delocalization, and thus enhances the conductivity of the composite polymer chain.

Wang et al. [59] prepared a polysiloxane–carbon nanotube (Si–MWNT) composite by polymerization of siloxane on the nan-

Table 1
Characteristics of hybrid polymer–carbon supports and electrocatalytic properties of supported catalysts.

Carbon type	Support	Support characteristics	Electrocatalytic properties of supported catalyst	References
Carbon blacks	PAni–C (IO)	Higher anti-poisoning ability than C.	Higher MOR activity and stability of Pt/PAni–C than Pt/C	[32]
	PAni–C (IO)	Higher electron and proton conductivities, methanol diffusion coefficient anti-poisoning ability than C.	Higher EAS, MOR activity and stability of Pt/PAni–C than Pt/C.	[33]
	PAni–C (OI)	Higher polymeric degree and a lower defect density in PAni–C than in PAni. Higher electron conductivity, and lower charge-transfer resistance than PAni.	Higher Pt dispersion and MOR activity of Pt/PAni–C than Pt/PAni	[35]
	NSA–PPy–C (IO)	Higher accessible surface area than C.	Higher Pt dispersion, HOR and MOR activity and stability of Pt/NSA–PPy–C than Pt/C	[34]
	PPy–C (IO and OI)	The thermal stability of PPy–C decrease with increasing PPy content	Lower ORR activity of Pt/PPy–C (IO)) than Pt/C. Similar ORR activity of Pt/PPy–C (OI) and Pt/PPy	[37]
Nanocarbons	PAni–SWNT (OI) and PAni–MWNT (OI)	Higher electron conductivity and porosity than PAni	Higher Pt dispersion and activity for methanol and formic acid oxidation of Pt/PAni–CNT than PAni	[47,48]
	PAni–SWNT (OI)	Higher polymeric degree and lower defect density than pure PAni. PAni film morphology significantly changed. Higher accessible surface areas, electronic conductivity and easier charge-transfer at polymer/electrolyte interfaces than PAni.	Higher Pt dispersion and activity for methanol and formaldehyde oxidation of Pt/PAni–SWNT than PAni	[49,50]
	PAni-f-MWNT (OI)	Higher accessible surface areas than PAni.	Higher Pt dispersion and activity for formic acid oxidation of Pt/PAni–CNT than PAni	[51]
	PAni-g-MWNT (IO)	Grafting of PANI on MWNT surfaces masks the defect sites in MWNT providing an uniform surface with positively charged sites.	Higher Pt dispersion and MOR activity of Au/PAni-g-MWNT than Au/MWNT	[52]
	PPy–MWNT (OI)	Higher accessible surface areas, electronic conductivity and easier charge-transfer at polymer/electrolyte interfaces than PPy.	Higher Pt dispersion and MOR activity of Pt/PPt-MWNT than Pt/PPy	[54]
	PPy–MWNT (IO)	PAni–MWNT show the tubular morphology of MWNT, in which the PPy is coated on each individual MWNT. The average diameter of the nanotubes increases with increasing PPy content in the composite.	Higher Pt dispersion and MOR activity of Pt/PPt-MWNT than Pt/MWNT	[55]
	PPy–MWNT (IO)	Change from the hydrophobic surface of MWNT to a hydrophilic PPy–MWNT surface.	Higher PtRu dispersion of PtRu/PPt-MWNT than PtRu/MWNT	[56]
	PAANI–MWNT	Higher accessible surface areas, electronic conductivity and easier charge-transfer at polymer/electrolyte interfaces than PAANI	Higher activity and stability for formaldehyde oxidation of Pt/PAANI-SWNT than PAANI.	[58]
	Si–MWNT	MWNT embedded within the polysiloxane shell. Chemical interactions between polysiloxane and MWNT. High proton conductivity.	Higher PtNi dispersion, MOR activity and stability of PtNi/S-MWNT than PtNi/MWNT	[59]

otube surfaces. The carbon nanotubes were embedded within the polysiloxane shell with a hydrophilic amino group situated outside. Then, PtNi nanoparticles were deposited on the Si–MWNT support by reduction of the adsorbed metal precursors with $NaBH_4$. FT-IR analysis of the purified Si–MWCNT composite indicated chemical interactions between the polysiloxane and the MWCNT. The electrocatalytic activity of the PtNi/Si–MWNT and PtNi/MWNT catalysts toward the oxidation of methanol was tested by CV measurements in a H_2SO_4/CH_3OH solution. The PtNi/Si–MWNT electrode showed a much lower onset potential and a higher current density than the PtNi/MWNT electrode, indicating a better electrocatalytic activity of PtNi/Si–MWNT electrode for methanol oxidation, which can be attributed to the high dispersion of PtNi catalysts and the effective functionalization of MWNT. The PtNi/Si–MWNT catalyst also showed a higher long-term stability than the PtNi/MWNT catalyst.

Fujigaya et al. [60] prepared a pyridine-containing polybenzimidazole (PyPBI) wrapped MWNT. PyPBI acts as an efficient dispersant for MWNT wrapping and produces a stable complex after removal of the unbound PyPBI. The wrapped PyPBI serve as the glue for immobilizing Pt nanoparticles onto the surface of MWCNT without any strong oxidation process for the MWCNT, often used to produce sites where metallic nanoparticles are immobilized. Based on this method, a highly homogeneous and remarkably efficient Pt loading onto the surface of MWCNT through a coordination reaction between Pt and PyPBI has been achieved. CV measurements revealed that the Pt nanoparticles deposited on the PyPBI-wrapped MWCNTs have a high electrochemically active surface area.

The characteristics of hybrid polymer–carbon supports and the electrocatalytic properties of supported catalysts are summarized in Table 1.

2.3. Dendrimer-encapsulated nanoparticles (DENs) supported on carbon

Dendrimers are monodisperse and highly branched macromolecules with highly ordered and controlled structures. Specifically, the structure and chemical properties of dendrimers can be logically controlled by modification of the core, the type and number of repetitive branch units, and the terminal functional groups. Crowding of surface functional groups on higher-generation dendrimers leads to a close-packed spherical periphery surrounding interior cavities. Different classes of dendrimers have been reported such as poly(propyleneimine) (PPI) dendrimers [61], poly(amidoamine) (PAMAM) dendrimers [62] and polyether dendrimers [63]. Four amine-terminated (G4–NH_2)

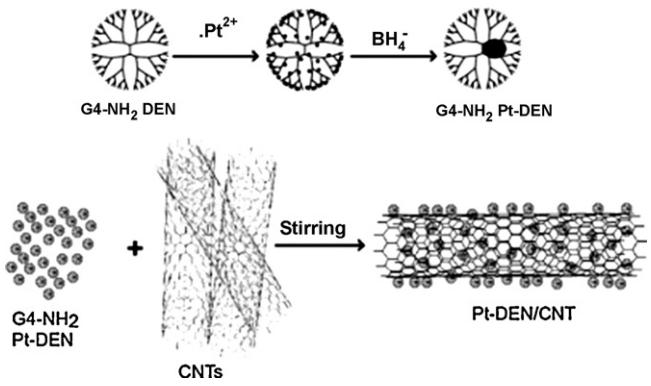

Fig. 4. Scheme of preparation of amine-terminated PAMAM–dendrimer-encapsulated Pt nanoparticles (G4–NH_2 Pt–DENs) and adsorption onto carbon nanotube supports.
Reproduced from Ref. [65], copyright 2007, with permission from the American Chemical Society.

and hydroxyl-terminated (G4–OH) dendrimers are approximately 4.5 nm in diameter and contain 62 interior tertiary amine groups and 64 peripheral functional groups. Dendrimers successfully stabilize nanoparticles, playing the role of a template (nanoparticles formed inside the dendrimer) or surfactants (nanoparticles formed between the dendrimers) [64].

Dendrimer-encapsulated nanoparticles are synthesized by complexing metal ions within dendrimers and then reducing the composites to yield zerovalent DENs [65–67], as shown in Fig. 4 from Ref. [65]. DENs are interesting, because they combine the desirable physical and chemical properties of the encapsulated nanoparticles with the tunable solubility and surface reactivity of the dendrimer template. Furthermore, the nanoparticle size, composition, and structure can be controlled by taking advantage of the dendrimer structure and the means by which the metal ions are introduced into the dendrimer [66]. The dendrimer also prevents aggregation of the nanoparticles without passivating all of the active sites on the nanoparticle surface. Among the other properties of DENs, it is easy to control the chemical composition of the peripheral groups on the dendrimer, and this provides a means for attaching DENs to supports and for solubilizing them in nearly any solvent. Moreover, the dendrimer periphery can function as a size-and-shape selective molecular filter, thereby providing a means for introducing selectivity to intrinsically nonselective metal catalysts [66]. The synthesis, characterization, and applications of DENs have been reviewed by Scott et al. [66].

PAMAM dendrimers in form of either G4–NH_2 [65,68] or G4–OH [69] have been used to encapsulate the catalyst and to anchor on the carbon substrate. Vijayaraghavan and Stevenson [65] described the use of a chemical vapor deposition (CVD) process to prepare nitrogen-doped carbon nanotube (N–CNT) supports, which strongly bind size-monodisperse Pt catalysts prepared by a dendrimer template method without the necessity for covalent or noncovalent functionalization of the carbon support prior to catalyst loading. The scheme of the preparation of CNT-supported DENs is shown in Fig. 4 from Ref. [65]. According to the authors, the choice of the PAMAM G4–NH_2 dendrimer template and terminal amine functional groups provides for uniform preparation of size-monodisperse catalysts and facilitates the controlled dispersion and loading of the catalysts onto N–CNT supports with well-controlled structural and compositional properties. The immersion-based loading of catalysts onto a carbon support by spontaneous adsorption to achieve specific Pt loadings offers a less aggressive processing approach for preparing carbon-supported catalysts compared to the harsher catalyst dispersion and loading methods that generally require oxidative treatment of the carbon support and/or chemical reduction of metal salts to achieve selective binding of the active metal catalyst. The activity for oxygen reduction of Pt–DENs/N–CNT with 7.5 at% N was similar to that of Pt/C.

Ye and Crooks [70] report a new strategy for DENs immobilization on glass carbon electrodes (GCEs) that is simple and that leads to robust, electrocatalytically active DEN monolayers. The approach involves preparation of DENs within hydroxyl-terminated dendrimers and subsequent coupling of the dendrimer to the GCE surface via an electro-oxidation reaction. On the basis of the method of Ye and Crooks [70], Ledesma-Garcia et al. [69] functionalized the surfaces of carbon-fiber for the purpose of obtaining activated surfaces. Then platinum-dendrimer nanocomposites (G4–OHPt) were anchored on the surface oxidized groups by cycling of the carbon-electrode potential. The degree of oxidation of the carbon surface affects the anchoring of the dendritic material, the coverage of which is indicated by the electroactive area of the encapsulated platinum. The modified carbon-fiber surfaces pretreated by cyclic polarization are found to be electrocatalytic for the ORR, presenting a good exchange-current density at low platinum loading.

Unlike the previous works, Mayalagan [68] first anchored the fourth-generation amine-terminated PAMAM dendrimers (G4–NH_2) on the functionalized carbon nanofiber as a substrate, and then encapsulated PtRu nanoparticles on dendrimers. The electrocatalytic activities for methanol oxidation of PtRu/DENs/CNF and commercial PtRu/C electrocatalysts were tested by cyclic voltammetry in an H_2SO_4/CH_3OH solution. The PtRu/DENs/CNF composite showed higher electrocatalytic activity for methanol oxidation compared to the PtRu/C catalyst. The enhanced catalytic activity of PtRu/PAMAM/CNF composite catalyst was ascribed to the higher dispersion of PtRu nanoparticles.

2.4. Carbon–ionomer supports

One of the most serious barriers for the widespread commercialization of direct methanol fuel cells (DMFCs) is the low electro-oxidation activity of methanol in the anode, needing a large amount of Pt or Pt-containing catalysts. Three transport processes are involved in the anodic electro-oxidation of methanol, that is, electron transport, proton transport and chemical species transport, thus an efficient electrode should maximize the three-phase boundary region. An effective electrocatalysts should be not only accessible to the reactants, but also electrically connected to the current collectors, and ionically connected to the electrolyte membrane. A typical DMFCs electrode is prepared by painting or spraying catalyst inks that contain the electrolyte (usually Nafion® ionomer) and the carbon-supported catalyst on either the gas diffusion layer or the electrolyte membrane [71]. Usually, the utilization of Pt is only about 20% [72] and the dispersion of the ionomer in the catalyst layer is not uniform. Watanabe et al. [73] reported that the catalyst layer of a PEMFC had two distinctive pore distributions with a boundary at *ca.* 100 nm. The smaller pore (primary pore) was identified with the space in and between the primary particles in the agglomerate, and the larger one (secondary pore) was that between the agglomerate. Uchida et al. [74] defined the pores from 20 to 40 nm to be the "primary pores," and the pores from 40 to 1000 nm the "secondary pores" in a PEMFC. The ionomer colloid consisted chiefly of the primary particles with a mean diameter about 43 nm. From these results, it should be emphasized that the ionomer added to the catalyst layer exists only in the secondary pores and not in the primary pores. They proposed that the secondary pores behaved as reaction sites in the PEMFC, because the ionomer electrolyte is present only in there. This suggested that the Pt particles loaded inside the agglomerate did not take part in the reaction, since the inside Pt particles were out of contact with the polymer electrolyte. On the other hand, the aggregation of the

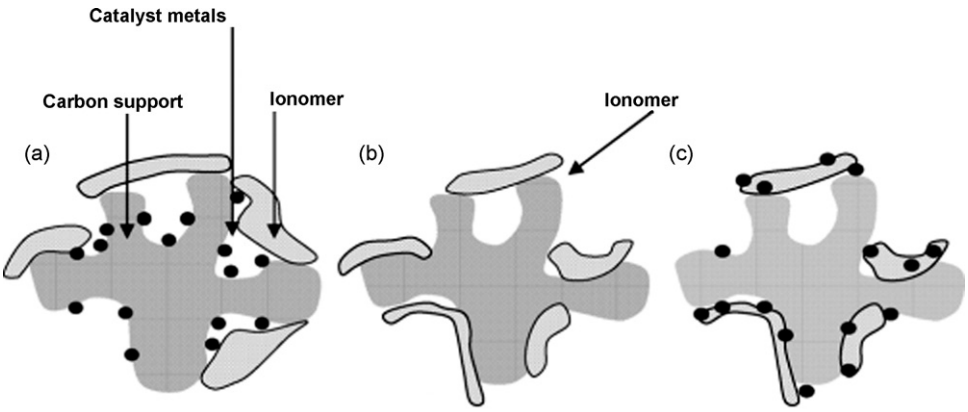

Fig. 5. Diagrammatic representation of: (a) catalyst–ionomer interaction in electrode using plain carbon as a support; (b) ionomer-coated carbon support; (c) catalyst–ionomer interaction on ionomer-coated carbon support.
Reproduced from Ref. [75], copyright 2006, with permission from Elsevier.

ionomer on the Pt particle surface will form a barrier to the reactants, lowering the electrochemically active sites of the catalyst. Therefore, these electrodes show poor electrolyte contact or poor reaction diffusion. A diagrammatic representation of this aspect is given in Fig. 5a from Park et al. [75]. The scheme shows that the interaction between the catalyst metal particles and the ionomer in the electrode is poor when plain carbon powder is employed as a support material.

To solve these problems, the electrolyte is first mixed with the carbon support to form carbon–Nafion® composites before the preparation of the catalyst. Mixed composites of Nafion® ionomer with carbon blacks [75,76], carbon gel [77] and carbon nanotubes [78] were prepared, then Pt or Pt–Ru catalysts were electrodeposited on the Nafion®-bonded carbons. Fig. 5b from Ref. [75] shows the ionomer-coated carbon support which is prepared by mixing the carbon powder with an perfluorosulfonic acid ionomer solution, followed by drying and crushing into fine powder. This modified carbon material offers an enhanced interfacial region with protonic continuum from the ionomer. Hence, a favorable and facilitating situation is readily available to the incoming catalyst particles while they are dispersed during catalyst preparation steps on such modified carbon support materials. Fig. 5c shows an improved catalyst–ionomer–carbon interaction, *i.e.*, a typical enhancement of the three-phase boundary required for an efficient reaction when the modified carbon material is used as a support, instead of a plain carbon. Consequently, a greater utilization of catalyst particles is also feasible. In conclusion, incorporation of ionomer in the carbon support enhances the contact area between the catalyst particles and ionomer and reduces the total amount of ionomer required in the anode catalyst layer. The reduced total ionomer content in the anode facilitates the mass transport of reactants and products. For all the types of carbons [75–78], catalysts dispersed on carbon supports coated with ionomer exhibited better performance than those on the plain carbon supports, owing to the increased interfacial area between catalyst particles and ionomer.

3. Composite ceramic–carbon supports

3.1. General overview

The most part of ceramic–carbon composites used in fuel cell catalysis are merely ceramic materials supported on a carbon substrate! The main role of the carbon is to stabilize highly dispersed ceramic nanoclusters, resulting in a high specific surface area [79]. Then, the catalyst is dispersed on this composite to maximize the interactions between the ceramic material and the metal catalyst. Composites with WO_3 [24,80–82], W_xC [83–87], TiO_2 [88,89], RuO_2 [90] and SnO_2 [91] as the ceramic materials supported on carbon blacks or carbon nanotubes are examples of carbon-supported ceramic materials used as substrates for fuel cell catalysts.

However, in some cases, mixed ceramic–carbon materials are true hybrid supports with improved properties other than the higher surface area of the ceramic compound, such as higher electron conductivity (by the presence of CNT) or higher corrosion resistance (by the presence of the oxide) than the single materials. The increase in the catalytic activity of catalysts supported on the hybrid ceramic–carbon composite was commonly ascribed to the synergic effect of the high electron conductivity of the carbon, particularly of carbon nanotubes, with the co-catalytic properties of the ceramic material.

3.2. Hybrid ceramic–carbon blacks supports

Very recently, two papers have been addressed to hybrid ceramic–carbon blacks supports, both with TiO_2 as the ceramic material [92,93]. TiO_2 has been extensively investigated as a fuel cell catalyst support due to its high corrosion stability in acidic environment [18]. Moreover, it is known that the hypo-d-oxides including TiO_2 have strong interaction with the hyper-d-electronic metals such as platinum, which results in the formation of intermetallic phases at the interphase between metal and support [94]. Therefore, it can be expected that the electronic structure of Pt would be favorably modified for the ORR by Ti species through a strong metal-support interaction. The major problems of the use of TiO_2 as fuel cell catalyst support, however, are its low specific surface area, limiting the metal loading on the support, and its poor electron conductivity.

Beak et al. [92] modified a commercially available carbon with TiO_2 precursors to use as a platinum support. Anatase TiO_2 nanoparticles (9 wt%) with a size of 3–5 nm were uniformly dispersed on the carbon support. An improved TiO_2–C dispersion in the aqueous solution of Pt precursor with respect to plain carbon, resulting in an improved Pt dispersion on TiO_2–C, was observed. This gave rise to a uniform distribution of Pt nanoparticles on the TiO_2–C support. The average particle sizes were 2.9, 2.6, and 3.1 nm for home made Pt/C, Pt/TiO_2–C and commercial Pt/C, respectively. It was also observed that the interactions between Pt and Ti species on TiO_2–C have an impact on the electronic state of Pt. The ORR activity of the Pt/TiO_2–C was higher than that of Pt/C in terms of both mass activity and specific activity. This result was attributed to both the higher surface area and the modified electronic structure of platinum.

Lee et al. [93] prepared nanostructures consisting of TiO_2 particles as a core and carbon as a shell (TiO_2@C) by heat treatment of TiO_2 nanoparticles at 700 or 900 °C in a methane atmosphere. The formation of TiO_2@C core–shell nanostructures takes place according to the reaction:

$$TiO_2 + CH_4 \rightarrow TiO_2 + C_{ads} + 2H_2 \rightarrow TiO_2@C \quad (1)$$

The thickness of carbon layers depends on the reaction temperature. The thickness of the shell in the sample heated at 700 °C (TiO_2@C-700) and 900 °C (TiO_2@C-900) was ~2 and ~4 nm, respectively. It is likely that the thicker layer of the TiO_2@C-900 than that of the TiO_2@C-700 results from the faster decomposition rate of CH_4 at 900 °C. The electrocatalytic activity and stability toward methanol electro-oxidation of the Pt/TiO_2@C catalysts was higher than that of Pt/Vulcan XC-72R. The enhancement in catalytic activity of the TiO_2@C-supported catalysts was attributed to the interactions between metal particles and core-shell supports. The higher electrochemical stability of the Pt/TiO_2@C than that of Pt/C was ascribed to the higher corrosion resistance of the TiO_2@C compared to Vulcan XC-72R.

3.3. Hybrid ceramic–CNT supports

A recent review by Eder [79] introduces inorganic–CNT hybrids as a new and very promising class of functional materials that combine the multiphase characteristics of nanocomposites with the synergistic functions of hybrid frameworks. In these materials, a synergistic effect arises through size domain effects and charge-transfer processes through the inorganic–CNT interface. This review provides a comprehensive description of the various synthesis approaches of ceramic–CNT hybrids and also demonstrates their outstanding potential for a wide range of applications concerning energy and the environment.

Nanostructured TiO_2 materials, with a typical dimension less than 100 nm, have recently emerged. Such materials include spheroidal nanocrystallite and nanoparticles together with (more recently synthesized) elongated nanotubes, nanosheets, and nanofibers [95]. In view of to their high stability, high surface area and moderate electrical conductivity, titanium dioxide nanotubes have been investigated as fuel cell catalyst support [18]. In particular, Maiyalagan et al. [96] found that the electrocatalytic activity of the platinum catalyst supported on TiO_2 nanotubes for methanol oxidation is found to be better than that of the standard commercial E-TEK catalyst. On this basis, He et al. [97] prepared CNT-modified nanotubular TiO_2 as a new support for Pt and Ru nanoparticles. Ni nanoparticles were electrodeposited inside the titania nanotubes as catalysts for the growth of carbon nanotubes via chemical vapor deposition (CVD) by decomposing acetylene. After removing the Ni catalysts, Ru and Pt nanoparticles were electrodeposited on the TiO_2–CNT support in sequence using chronopotentiometry. TiO_2 nanotubes presented a pore size of about 90 nm in diameter and a length of about 320 nm. CNTs in diameter of 90 nm were formed on TiO_2 substrate. The TiO_2 substrate, after removing the surface CNTs of the TiO_2–CNTs electrode, showed a CNTs-embedded porous annealed TiO_2 substrate, due to formation of CNTs inside the TiO_2 nanotubes at 650 °C before the distortion of the titania nanotubes at 680 °C. Such a CNTs-embedded TiO_2 substrate facilitates the electron transfer due to its enhanced conductivity. The TiO_2 nanotubes were disintegrated during the CNT growing process at 700 °C, existing in the mixture of rutile and anatase phase. The electrocatalytic activity of PtRu/TiO_2–CNT was investigated with respect to the methanol oxidation in H_2SO_4 solutions. As compared with a graphite substrate, TiO_2 substrate displays a higher catalytic activity for the MOR. The high catalytic activity was ascribed to the large surface area of CNT network, the conductive CNT-embedded TiO_2 substrate, the uniformly distributed Pt and Ru nanoparticles, and the synergistic catalytic action of TiO_2.

SnO_2 has been proposed as a support material for fuel cell electrocatalysts because of its chemical properties: it adsorbs OH species at low potentials and/or induces the electronic effect with Pt catalysts [18]. These properties promote the electro-oxidation on Pt of CO [98] and low-molecular-weight alcohol, such as methanol [99] and ethanol [22]. For its use as a catalyst support in fuel cells, however, the electrical conductance of SnO_2 has to be improved. Indeed, undoped tin dioxide is a wide bandgap semiconductor ($E_g \sim 3.6$ eV) with electrical resistivity varying from 10 to 10^6 Ω cm, depending on the temperature and the stoichiometry of the oxide [100]. The problem of the low electronic conductivity of tin oxide regarding its use as fuel cell catalyst support can be overcome by using metal-doped SnO_2 [101,102] or by mixing SnO_2 with a highly conductive carbon material, such as carbon nanotubes [103–105].

Pang et al. [103] and Hsu et al. [104] prepared SnO_2–CNT composites with different mass ratio of CNTs to SnO_2 (R_{CNT/SnO_2}), either by adding the carbon nanotubes to a tin oxide matrix [103] or by adding SnO_2 to SWNT [104]. Then, platinum was deposited on these hybrid supports, and the electrocatalytic activity of the Pt/SnO_2–CNT catalysts for ethanol oxidation was investigated. The Pt/SnO_2–CNTs catalysts showed higher electrocatalytic activity than the Pt/SnO_2 catalyst [103] and the Pt/SWNT catalyst [104]. The effect of the mass ratio of CNT to SnO_2 on the electrocatalytic activity of the electrode for ethanol oxidation was investigated: an optimum mass ratio of 1/6.3 of CNT to SnO_2 in the Pt/SnO_2–CNT catalysts prepared by adding CNT to SnO_2, and an optimum mass ratio of 50:1 of precursor salt ($SnCl_2{\cdot}2H_2O$) in the Pt/SnO_2–CNT catalysts prepared by adding tin oxide to carbon nanotubes, were observed. The effect of the mass ratio in the SnO_2–CNTs composites on the electrocatalytic activity of the Pt/SnO_2–CNTs catalyst is shown in Fig. 6a from Ref. [103]. It can be observed that the peak current densities of ethanol oxidation at the Pt/SnO_2–CNTs catalysts are all higher than that at the Pt/SnO_2 catalyst. According to the results in Fig. 6a and b presents the plot of the current density of peak I against the value of R_{CNT/SnO_2}. As can be observed in Fig. 6b, the current density of peak I of ethanol oxidation at the Pt/SnO_2–CNTcatalyst goes trough a maximum at $R_{CNT/SnO_2} = 1/6.3$. This may explain as follows: compared with pure SnO_2 particles, a certain amount of CNT can improve the electrocatalytic activity of the Pt/SnO_2 catalyst. The introduction of CNT improves the conductivity of the Pt/SnO_2–CNTs/graphite electrode, which is beneficial to the electrochemical oxidation of ethanol. On the other hand, under the same mass of the SnO_2–CNT composites, a further increase of the content of CNT will result in the decrease of the content of SnO_2. In this case, there will be less active sites of SnO_2 to form oxygen-containing species, which is harmful for improving the electrocatalytic activity of the Pt/SnO_2–CNTs catalyst.

Du et al. [105] prepared a mesoporous SnO_2 coated carbon nanotube core-sheath nanocomposite, CNT@SnO_2, by a hydrothermal method and proposed it as a catalyst support for PEMFCs. To examine the electrochemical stability of the CNT@SnO_2, Fig. 7 from Ref. [104] shows the steady-state corrosion currents at different potentials for the CNT@SnO_2, the CNT and the SnO_2, which was prepared by the same procedure as the CNT@SnO_2 except that no CNT was added. For SnO_2, the corrosion current at all potentials was almost negligible, suggesting that SnO_2 had sufficient electrochemical stability, even at high potentials. For CNT@SnO_2 and CNT, at relatively low potentials, the corrosion currents were small, showing that the two materials were both stable. However, at high potentials beyond 1.4 V, the corrosion current for CNT increased rapidly with increasing the potential. In contrast, only a small increase in the corrosion current was observed for CNT@SnO_2 up to 1.8 V. At these corrosion rates, about 20% weight loss would appear for the CNT in 10 h at 1.5 V, while only 1.4% for the case of CNT@SnO_2. This fact

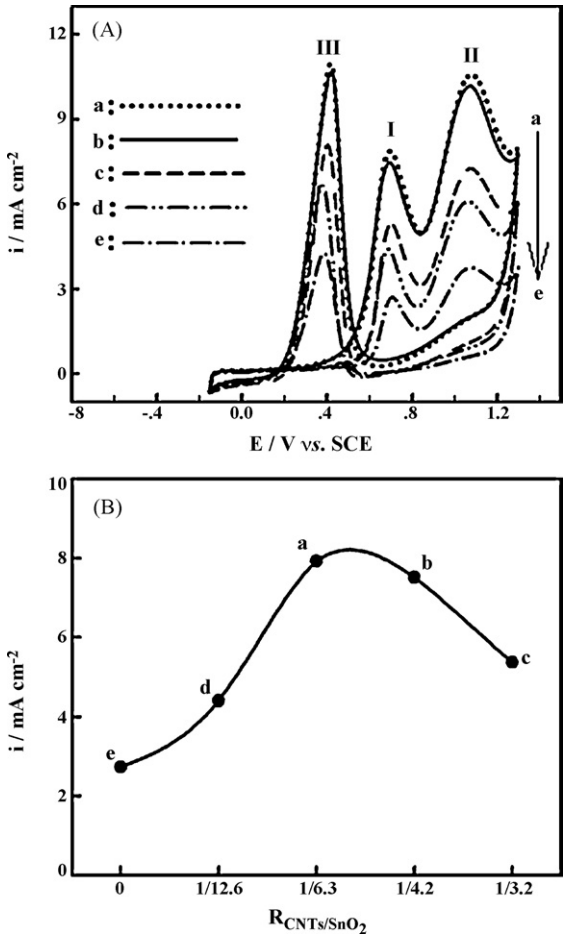

Fig. 6. (A) Cyclic voltammograms of ethanol oxidation at the Pt/SnO_2–CNT graphite electrodes with different molar ratio of CNT to SnO_2 (). (a) $R_{CNT/SnO_2} = 1/6.3$; (b) $R_{CNT/SnO_2} = 1/4.2$; (c) $R_{CNT/SnO_2} = 1/3.2$; (d) $R_{CNT/SnO_2} = 1/12.6$; (e) $R_{CNT/SnO_2} = 0$. (B) The dependence of the current density of peak I at the Pt/SnO_2–CNT/graphite electrode on R_{CNT/SnO_2}. Mass loading of Pt = 19.4 μg cm^{-2}.
Reproduced from Ref. [103], copyright 2009, with permission from Elsevier.

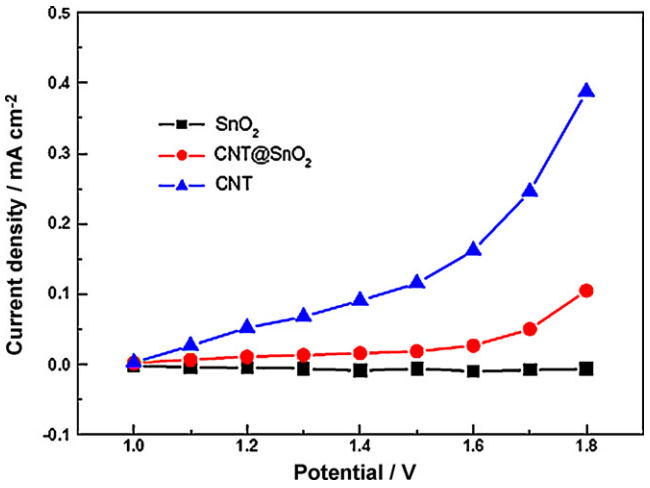

Fig. 7. Steady-state corrosion currents of the CNT@SnO_2, SnO_2 and CNT in N_2-purged 0.5 M H_2SO_4 solution as a function of polarization potential.
Reproduced from Ref. [104], copyright 2009, with permission from Elsevier.

clearly indicated that the CNT@SnO_2 was more oxidation-resistant and durable than the CNT under the PEMFC operating conditions. The Pt/(CNT@SnO_2) catalyst was electrochemically active and exhibited comparable activity for the ORR to the CNT-supported catalyst (Pt/CNT). More importantly, the long-term stability of the Pt/(CNT@SnO_2) catalyst was significantly higher than that of the Pt/CNT catalyst, which might be mainly due to the fact that the CNT@SnO_2 was more corrosion resistant and mesoporous SnO_2 was beneficial to restrict the Pt migration and aggregation.

MnO_2 nanotubes [106] and MnO_2 nanowires [107] have been used as supports for Pd and Pt catalysts, respectively. Pd/MnO_2 nanotubes and Pt/MnO_2 nanowires showed a higher activity for methanol oxidation than Pd/C and Pt nanowires, respectively. However, the preparation of MnO_2 nanotubes or nanowires is a relatively complex and costly course, and the use of the common MnO_2 compound as catalyst support is hindered by its poor electric conductivity. Thus, Zhou et al. [108] synthesized $MnO_2 \cdot xH_2O$/CNTs and used to support Pt and PtRu as DMFC catalysts. $MnO_2 \cdot xH_2O$ in the support is capable of increasing the proton conductivity and Pt utilization of the catalysts and then improving the performance for methanol electro-oxidation. Pt/MnO_2–CNTs and PtRu/MnO_2–CNTs presented high electrochemical active surface area and superior methanol electro-oxidation activity than Pt/CNT and PtRu/CNT, respectively.

The characteristics of hybrid ceramic–carbon supports and the electrocatalytic properties of supported catalysts are summarized in Table 2.

4. Composite polymer–ceramic supports

A newly emerging area of materials, called “nanohybrid” or “nanocomposite” materials, results from the tuning of molecular level interactions of dissimilar organic and inorganic components to form new unique functional materials with improved properties. This approach has been successfully used recently for the synthesis of novel nanocomposite materials by a redox interca-

Table 2
Characteristics of hybrid ceramic–carbon supports and electrocatalytic properties of supported catalysts.

Carbon type	Support	Support characteristics	Electrocatalytic properties of supported catalyst	References
Carbon blacks	TiO_2–C	Improved TiO_2–C dispersion in the aqueous solution of Pt precursor with respect to plain carbon,	Modification of Pt electronic structure by Ti. Higher Pt dispersion and ORR activity of Pt/TiO_2–C than Pt/C.	[92]
Nanocarbons	TiO_2@C	Higher corrosion resistance of the TiO_2@C compared to Vulcan XC-72R.	Higher MOR activity and stability of Pt/TiO_2@C than Pt/C.	[93]
	TiO_2–CNT	CNTs-embedded porous annealed TiO_2 substrate. CNTs-embedded TiO_2 substrate facilitates the electron transfer due to its enhanced conductivity.	Higher MOR activity of PtRu/TiO_2–CNT than PtRu/TiO_2–C.	[97]
	SnO_2–CNT	Higher electronic conductivity than SnO_2	Higher EOR activity of Pt/SnO_2–CNT than Pt/SnO_2.	[103]
	SnO_2–SWNT	Higher thermal stability than SWNT	Higher EOR activity of Pt/SnO_2–SWNT than Pt/SWNT	[104]
	SnO_2@CNT	Higher corrosion resistance than CNT.	Same ORR activity, higher stability of Pt/SnO_2@CNT than Pt/CNT.	[105]
	MnO_2–CNT	Higher surface area and proton conductivity than CNT.	Higher MOR activity of Pt/MnO_2–CNT than Pt/CNT.	[106]

Table 3
Characteristics of hybrid polymer–ceramic supports and electrocatalytic properties of supported catalysts.

Support	Support characteristics	Electrocatalytic properties of supported catalyst	References
PAni–V_2O_5	Higher stability of PAni–V_2O_5 compared to the individual components.	Higher MOR activity and stability of Pt/PAni–V_2O_5 than bulk Pt.	[116]
PEDOT–V_2O_5	Continuous and relatively homogeneous matrix with a distinct lamellar morphology. No bulk deposition of polymer on the surface of the microcrystallites.	Higher MOR activity and stability of Pt/PEDOT–V_2O_5 than Pt/C.	[117]
PAni–SnO_2	Lower polymer crystallinity in PAni–SnO_2 than in plain PAni.	Higher MOR activity and stability of Pt/PAni–SnO_2 than Pt/SnO_2.	[118]

lation strategy to prepare hybrid lamellar transition-metal oxides having enhanced synergic activity [109–112,31]. It is well known that intercalation leads to changes in the interlayer spacing for layered materials. For example, several conducting polymers such as PAni, PPy and PTh are known to oxidatively polymerize when intercalated into highly oxidizing transition-metal oxides such as V_2O_5. Several recent reports focus on specific preparation of conducting polymer nanocomposites and their functional properties particularly on the possibility of enhancing the energy storage characteristics for lithium batteries [113–115]. Only very recently polymer–ceramic composites have been explored as fuel cell catalyst supports [116–118].

Rajesh et al. [116] prepared a PAni–V_2O_5 nanocomposite material via the intercalation of polyaniline in V_2O_5 matrix by direct chemical oxidation of aniline16 (*i.e.*, *in situ* oxidative polymerization of aniline) using V_2O_5 xerogel. The interlayer expansion of the V_2O_5 layers from XRD analysis confirmed the formation of an intercalated compound. CV measurements indicated higher stability of PAni–V_2O_5 compared to the individual components. The enhanced stability of the composite was ascribed to the interaction between the organic component and the inorganic oxide. PAni–V_2O_5 was used as the support for Pt in methanol oxidation reaction. The average particle size of the Pt was 4 nm. The activity for methanol oxidation and stability of the Pt/PAni–V_2O_5 electrode was higher than that of bulk Pt electrode. Although the activity was fairly high for the present loading of Pt, the activity could be further increased. The probable reason for this is the conductivity of the nanocomposite system. The conductivity of the nanocomposite system might be higher than the crystalline V_2O_5, but the method of the intercalation of the polymer reduces the polymer conductivity, which might affect the charge-transfer at the electrode/electrolyte interface.

On the basis of the work of Murugan et al. [113], Maiyalagan and Viswanathan [117] used a stable conducting poly(3,4-ethylenedioxythiophene) (PEDOT)–V_2O_5 nanocomposite as a support for Pt. The electrocatalytic activity of Pt/PEDOT–V_2O_5 toward methanol oxidation was higher than that of a commercially available Pt/C catalyst. Fig. 8 from Ref. [115] shows the chronoamperometric response of Pt/PEDOT–V_2O_5 and Pt/C electrodes at a constant potential of +0.6 V versus Ag/AgCl in 1 M H_2SO_4 and 1 M CH_3OH. The methanol oxidation activity and the stability for Pt/PEDOT–V_2O_5 nanocomposite based electrode were higher than that of Pt/C electrode. The porous PEDOT–V_2O_5 nanocomposite leads to the high dispersion of Pt particles on its surface and also the porous morphology of the nanocomposite is favorable for the transport of methanol in the catalyst layer. The conducting poly(3,4-ethylenedioxythiophene) not only acted as an excellent electronic support for Pt particles but also increased the stability of the layered transition-metal oxide, under the electrochemical operating conditions.

Pang et al. [118] prepared PAni–SnO_2 composites by chemical polymerization of aniline in the presence of SnO_2. Then platinum was supported on this hybrid material and on SnO_2 for comparison. XRD diffraction peaks of pure PAni were not observed in the XRD pattern of the PAni–SnO_2 composites, indicating that SnO_2 nanoparticles hamper the crystallization of PAni. Pt nanoparticles were dispersed uniformly on the PAni–SnO_2 composites. Pt particle size in the Pt/PAni–SnO_2 (about 3.2 nm) was lower than that in the Pt/SnO_2 catalyst (4.3 nm). Comparing with the Pt/SnO_2/GC electrode, the Pt/PAni–SnO_2/GC electrode showed better electrochemical performance (larger ESA, higher electrocatalytic activity for methanol oxidation and better anti-poisoning ability) under the same experimental conditions.

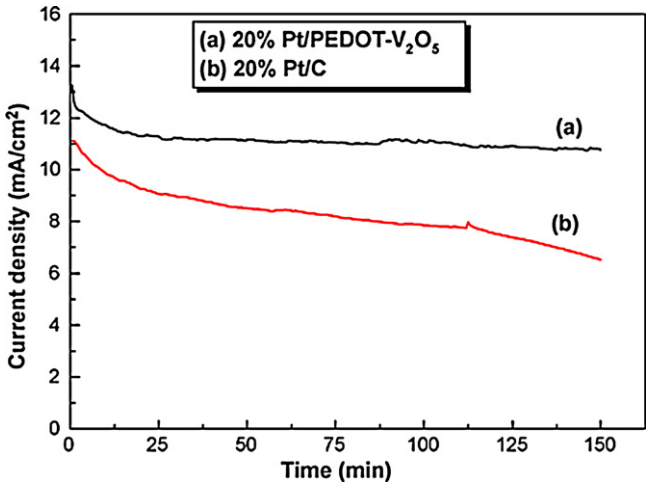

Fig. 8. Chronoamperometric response of (a) Pt/PEDOT–V_2O_5 nanocomposite electrodes and (b) Pt/C polarized at +0.6 V in 1 M H_2SO_4/1 M CH_3OH.
Reproduced from Ref. [117], copyright 2010, with permission from Elsevier.

The characteristics of hybrid polymer–ceramic supports and the electrocatalytic properties of supported catalysts are summarized in Table 3.

5. Conclusions

Since plain carbon, ceramic and polymer materials are not completely satisfactory, composite materials have been investigated as fuel cell catalyst supports. The most studied hybrid materials as fuel cell catalyst supports were polymer–carbon composites, followed by ceramic–carbon composites, and, very recently, by polymer–ceramic composites. These hybrid materials possess the properties of each component, and even a synergistic effect.

Generally, regarding the hybrid polymer–carbon materials, the type of material (IO or OI) is related to the type of carbon used in the composite. Polymer is commonly added to carbon blacks to improve the characteristics of the carbon (IO materials), in particular to increase the accessible surface area and to decrease the catalyst susceptibility to poisoning. Conversely, carbon nanotubes are added to the polymer matrix (OI materials) overall to increase its conductivity and stability.

The polymer is commonly prepared by polymerization of the monomer in the presence of carbon. The presence of carbon promotes the rate of aniline polymerization, resulting in a higher polymeric degree and a lower defect density in the polymer structure. Hybrid polymer–carbon supports present higher

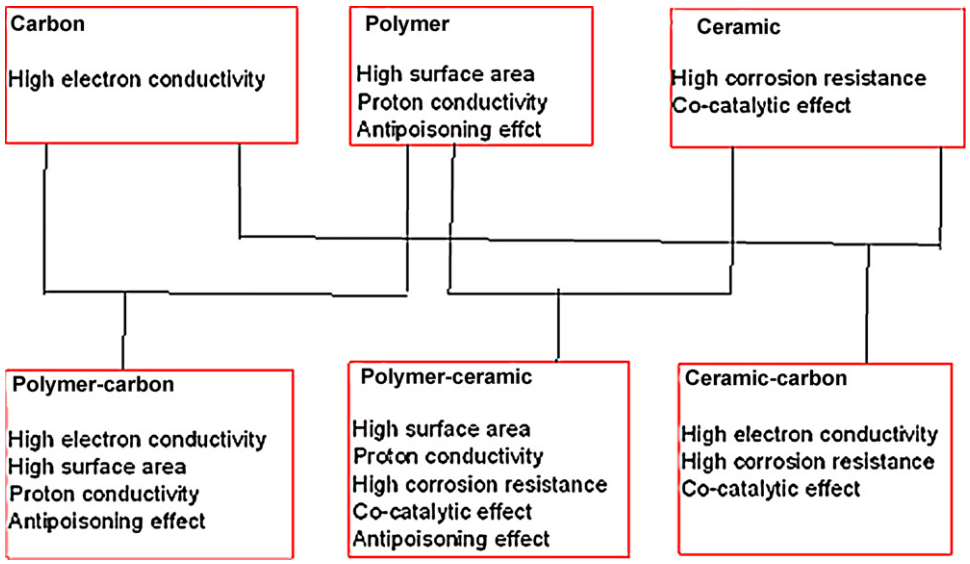

Fig. 9. Scheme showing the main characteristics of plain and hybrid material supports.

accessible surface areas, higher electronic conductivity and easier charge-transfer at the polymer/electrolyte interface than the single matrix. The size of the metal nanoparticles deposited on the polymer–carbon composite matrix is commonly smaller than that on single polymer. This results in a higher dispersion and better utilization of the metal nanoparticle-impregnated composites. The higher catalyst dispersion, together with the enhanced properties of the hybrid support, results in a high performance of the composite-supported catalysts. Indeed, the electrocatalytic activity of almost all of polymer–carbon composites is higher than that of pristine polymer (OI materials) or pristine carbon (IO materials).

In the hybrid ceramic–carbon materials, the ceramic material supplies co-catalytic properties and increases the corrosion resistance, and the carbon supplies a high electron conductivity to the mixed composite.

Finally, in the hybrid polymer–ceramic materials, the polymer confers a high surface area and proton conductivity, and the inorganic high corrosion resistance and co-catalytic activity to the composite.

The scheme reported in Fig. 9 shows the main characteristics of plain and hybrid material supports. In addition to the sum of the properties of the individual components, indicated in the scheme, synergic properties, which not belong to the single component, are present in the mixed composites, such as a higher polymeric degree and lower defect density in the polymer structure [37,51], and a higher degree of porosity of the composite [50,52].

Dendrimer-encapsulated nanoparticles and ionomer coated are mixed polymer–carbon materials, where the function of the polymer is to stabilize the nanoparticles and to enhance the three-phase boundary, respectively, while the carbon acts as the support.

Apart carbon-ionomer supports, which were tested also in fuel cells, all the electrochemical tests on these mixed supports have been carried out in liquid environment such as H_2SO_4 or $HClO_4$. To confirm the excellent results obtained by electrochemical measurements such as cyclic voltammetry and chronoamperometry, tests in a membrane electrode assembly (MEA) have to be carried out to evaluate their catalytic activity in practical applications.

It is important to remark that the exploration of these composite materials as suitable fuel cell catalyst supports is only at the beginning: indeed, the first communication addressed to this issue appearing in the year 2005 by Wu et al. [37]. So, further attempts have to be made to design and synthesize composite polymer–carbon, ceramic–carbon and polymer–ceramic materials to improve their properties as electrocatalyst supports. There is still much room regarding the optimization of the type of mixed materials, the relative ratio and the structure of the materials. A question is what the next fillers will be for polymers, and the answer might well be more high aspect ratio, nanoscale fillers, such as nanorods and nanowires [41]. On the basis of the significant progress in the understanding of these composite systems and the promising results of preliminary tests, the hybrid materials represent the right way for the development of improved supports for fuel cell catalysts.

Acknowledgment

The author thanks the Conselho Nacional de Desenvolvimento Científico e Tecnológico (CNPq, Proc. 310151/2008-2) for financial assistance to the project.

References

[1] P. Costamagna, S. Srinivasan, J. Power Sources 102 (2001) 242–252.
[2] S. Wasmus, A. Küver, J. Electroanal. Chem. 461 (1999) 14–31.
[3] E. Antolini, J. Power Sources 170 (2007) 1–12.
[4] E. Antolini, Mater. Chem. Phys. 78 (2003) 563–573.
[5] E. Antolini, Appl. Catal. B 88 (2009) 1–24.
[6] A.M. Couper, D. Pletcher, F.C. Walsh, Chem. Rev. 90 (1990) 837–865.
[7] G.A. Gruver, J. Electrochem. Soc. 125 (1978) 1719–1720.
[8] P. Stonehart, Carbon 22 (1984) 423–431.
[9] J. McBreen, H. Olender, S. Srinivasan, K.V. Kordesch, J. Appl. Electrochem. 11 (1981) 787–796.
[10] K.H. Kangasniemi, D.A. Condit, T.D. Jarvi, J. Electrochem. Soc. 151 (2004) E125–E132.
[11] R.L. Borup, J.R. Davey, F.H. Garzon, D.L. Wood, M.A. Inbody, J. Power Sources 163 (2006) 76–81.
[12] J. Wang, G. Yin, Y. Shao, S. Zhang, Z. Wang, Y. Gao, J. Power Sources 171 (2007) 331–339.
[13] A. Taniguchi, T. Akita, K. Yasuda, Y. Miyazaki, J. Power Sources 130 (2004) 42–49.
[14] L.M. Roen, C.H. Paik, T.D. Jarvi, Electrochem. Sol. State Lett. 7 (2004) A19–22.
[15] T. Maiyalagan, B. Viswanathan, U.V. Varadaraju, Electrochem. Commun. 7 (2005) 905–912.
[16] A. Kongkanand, S. Kuwubata, G. Girishkumar, P. Kamat, Langmuir 22 (2006) 2392–2396.
[17] X. Wang, W. Li, Z. Chen, M. Waje, Y. Yan, J. Power Sources 158 (2006) 154–159.
[18] E. Antolini, E.R. Gonzalez, Solid State Ionics 180 (2009) 746–763.
[19] J.W. Long, R.M. Stroud, K.E. Swider-Lyons, D.R. Rolison, J. Phys. Chem. B 104 (2000) 9772–9776.
[20] Q. Lu, B. Yang, L. Zhuang, J. Lu, J. Phys. Chem. B 109 (2005) 1715–1722.
[21] L. Jiang, G. Sun, S. Sun, J. Liu, S. Tang, H. Li, B. Zhou, Q. Xin, Electrochim. Acta 50 (2005) 5384–5389.

[22] L. Jiang, L. Colmenares, Z. Jusys, G.Q. Sun, R.J. Behm, Electrochim. Acta 53 (2007) 377–389.
[23] K.-W. Park, K.-S. Ahn, Y.-C. Nah, J.-H. Choi, Y.-E. Sung, J. Phys. Chem. B 107 (2003) 4352–4355.
[24] V. Raghuveer, B. Viswanathan, J. Power Sources 144 (2005) 1–10.
[25] E. Antolini, E.R. Gonzalez, Appl. Catal. A 365 (2009) 1–19.
[26] Z. Qi, P.G. Pickup, Chem. Comm (1998) 15–16.
[27] C.T. Hable, M.S. Wrighton, Langmuir 9 (1993) 3284–3289.
[28] Yu.M. Maksimov, E.A. Kolyadko, A.V. Shishlova, B.I. Podlovchenko, Russian J. Electrochem. 37 (2001) 777–785.
[29] G. Wu, L. Li, J.H. Li, B.Q. Xu, J. Power Sources 155 (2006) 118–127.
[30] P. Gomez-Romero, Adv. Mater. 13 (2001) 163–174.
[31] D.J. Cardin, Adv. Mater. 14 (2002) 553–563.
[32] Y. Xu, X. Peng, H. Zeng, L. Dai, H. Wu, C. R. Chim. 11 (2008) 147–151.
[33] H. Gharibi, K. Kakaei, M. Zhiani, J. Phys. Chem. C 114 (2010) 3956–3961.
[34] H. Zhao, L. Li, J. Yang, Y. Zhang, J. Power Sources 184 (2008) 375–380.
[35] G. Wu, L. Li, J.-H. Li, B.-Q. Xu, Carbon 43 (2005) 2579–2587.
[36] H. Zhao, L. Li, J. Yang, Y. Zhang, H. Li, Electrochem. Commun. 10 (2008) 876–879.
[37] S. Mokrane, L. Makhloufi, N. Alonso-Vante, J. Solid State Electrochem. 12 (2008) 569–574.
[38] M. Terrones, Ann. Rev. Mater. Res. 33 (2003) 419–501.
[39] M. Moniruzzaman, K.I. Winey, Macromolecules 39 (16) (2006) 5194–5205.
[40] S. Roche, Ann. Chim. Sci. Mater. 25 (2000) 529–532.
[41] S. Niyogi, M.A. Hamon, H. Hu, B. Zhao, P. Bhowmik, R. Sen, M.E. Itkis, R.C. Haddon, Acc. Chem. Res. 35 (2002) 1105–1113.
[42] S. Bose, R.A. Khare, P. Moldenaers, Polymer 51 (2010) 975–993.
[43] N.G. Sahoo, S. Rana, J.W. Cho, L. Li, S.H. Chan, Prog. Polym. Sci. 35 (2010) 837–867.
[44] J.-C. Chiang, A.G. MacDiarmid, Synt. Met. 13 (1986) 193–205.
[45] P. Gajendran, R. Saraswathi, Pure Appl. Chem. 80 (2008) 2377–2395.
[46] J. Deng, X. Ding, W. Zhang, Y. Peng, J. Wang, X. Long, P. Li, A.S.C. Chan, Eur. Polym. J. 38 (2002) 2497–2501.
[47] J. Shi, D. Guo, Z. Wang, H. Li, J. Solid State Electrochem. 9 (2005) 634–638.
[48] J. Shi, Z. Wang, H. Li, J. Mater. Sci. 42 (2007) 539–544.
[49] G. Wu, L. Li, J.-H. Li, B.-Q. Xu, J. Power Sources 155 (2006) 118–127.
[50] Z. Wang, Z.-Z. Zhu, J. Shi, H.-L. Li, Appl. Surf. Sci. 253 (2007) 8811–8817.
[51] Z.-Z. Zhu, Z. Wang, H.-L. Li, Appl. Surf. Sci. 254 (2008) 2934–2940.
[52] P. Santhosh, A. Gopalan, K.-P. Lee, J. Catal. 238 (2006) 177–185.
[53] V. Selvaraj, M. Alagar, K.S. Kumar, Appl. Catal. B 75 (2007) 129–138.
[54] V. Selvaraj, M. Alagar, Electrochem. Commun. 9 (2007) 1145–1153.
[55] B. Qu, Y.-T. Xu, S.-j. Lin, Y.-F. Zheng, L.-Z. Dai, Synth. Met. 160 (2010) 732–742.
[56] H.-B. Bae, J.-H. Ryu, B.-S. Byun, S.-H. Jung, S.-H. Choi, Curr. Appl. Phys. 10 (2010) S44–S50.
[57] C. Jiang, X. Lin, J. Power Sources 164 (2007) 49–55.
[58] C. Jiang, H. Chen, C. Yu, S. Zhang, B. Liu, J. Kong, Electrochim. Acta 54 (2009) 1134–1140.
[59] Z.-C. Wang, Z.-M. Ma, H.-L. Li, Appl. Surf. Sci. 254 (2008) 6521–6526.
[60] T. Fujigaya, M. Okamoto, N. Nakashima, Carbon 47 (2009) 3227–3232.
[61] E. Buhleier, W. Wehner, F. Vogtle, Synthesis (1978) 155–158.
[62] D.A. Tomalia, A.M. Naylor, W.A. Goddard, Angew. Chem. Int. Ed. Engl. 29 (1990) 138–175.
[63] C.J. Hawker, J.M.J. Frechet, J. Am. Chem. Soc. 112 (1990) 7638–7647.
[64] L.M. Bronstein, Z.B. Shifrina, Nanotechnol. Russ. 4 (2009) 576–608.
[65] G. Vijayaraghavan, K.J. Stevenson, Langmuir 23 (2007) 5279–5282.
[66] R.W.J. Scott, O.M. Wilson, R.M. Crooks, J. Phys. Chem. B 109 (2005) 692–704.
[67] R.W.J. Scott, H. Ye, R.R. Henriquez, R.M. Crooks, Chem. Mater. 15 (2003) 3873–3878.
[68] T. Maiyalagan, J. Solid State Electrochem. 13 (2009) 1561–1566.
[69] J. Ledesma-García, I.L. Escalante García, F.J. Rodríguez, T.W. Chapman, L.A. Godínez, J. Appl. Electrochem. 38 (2008) 515–522.
[70] H. Ye, R.M. Crooks, J. Am. Chem. Soc. 127 (2005) 4930–4934.
[71] E. Antolini, J. Appl. Electrochem. 34 (2004) 563.
[72] E.A. Ticianelli, C.R. Derouin, S. Srinivasan, J. Electroanal. Chem. 251 (1988) 275–295.
[73] M. Watanabe, M. Tomikawa, S. Motoo, J. Electroanal. Chem. 195 (1985) 81–93.
[74] M. Uchida, Y. Fukuoka, Y. Sugawara, N. Eda, A. Ohta, J. Electrochem. Soc. 143 (1996) 2245–2252.
[75] C.H. Park, M.A. Scibioh, H.-J. Kim, I.-H. Oh, S.-A. Hong, H.Y. Ha, J. Power Sources 162 (2006) 1023–1028.
[76] M.A. Scibioh, I.-H. Oh, T.-H. Lim, S.-A. Hong, H.Y. Ha, Appl. Catal. B 77 (2008) 373–385.
[77] C. Arbizzani, S. Beninati, E. Manferrari, F. Soavi, M. Mastragostino, J. Power Sources 161 (2006) 826–830.
[78] S. Chen, F. Ye, W. Lin, J. Nat. Gas Chem. 18 (2009) 199–204.
[79] D. Eder, Chem. Rev. 110 (2010) 1348–1385.
[80] F. Maillard, E. Peyrelade, Y. Soldo-Olivier, M. Chatenet, E. Chaînet, R. Faure, Electrochim. Acta 52 (2007) 1958–1967.
[81] Z. Zhang, X. Wang, Z. Cui, C. Liu, T. Lu, W. Xing, J. Power Sources 185 (2008) 941–945.
[82] J. Ye, J. Liu, Z. Zou, J. Gu, T. Yu, J. Power Sources 195 (2010) 2633–2637.
[83] R. Venkataraman, H.R. Kunz, J.M. Fenton, J. Electrochem. Soc. 150 (2003) A278–A284.
[84] M. Nie, P.K. Shen, M. Wu, Z. Wei, H. Meng, J. Power Sources 162 (2006) 173–176.
[85] L.G.R.A. Santos, K.S. Freitas, E.A. Ticianelli, J. Solid State Electrochem. 11 (2007) 1541–1548.
[86] M.K. Jeon, K.R. Lee, W.S. Lee, H. Daimon, A. Nakahara, S.I. Woo, J. Power Sources 185 (2008) 927–931.
[87] F. Hu, G. Cui, Z. Wei, P.K. Shen, Electrochem. Commun. 10 (2008) 1303–1306.
[88] H. Song, X. Qiu, F. Li, W. Zhu, L. Chen, Electrochem. Commun. 9 (2007) 1416–1421.
[89] D.-J. Guo, X.-P. Qiu, L.-Q. Chen, W.-T. Zhu, Carbon 47 (2009) 1680–1685.
[90] L. Cao, F. Scheiba, C. Roth, F. Schweiger, C. Cremers, U. Stimming, H. Fuess, L. Chen, W. Zhu, X. Qiu, Angew. Chem. Int. Ed. 45 (2006) 5315–5319.
[91] J. Parrondo, F. Mijangos, B. Rambabu, J. Power Sources 195 (2010) 3977–3983.
[92] S. Beak, D. Jung, K.S. Nahm, P. Kim, Catal. Lett. 134 (2010) 288–294.
[93] J.-M. Lee, S.-B. Han, J.-Y. Kim, Y.-W. Lee, A.-R. Ko, B. Roh, I. Hwang, K.-W. Park, Carbon 48 (2010) 2290–2296.
[94] N.V. Krstajic, L.M. Vracar, V.R. Radmilovic, S.G. Neophytides, M. Labou, J.M. Jaksic, R. Tunold, P. Falaras, M.M. Jaksic, Surf. Sci. 601 (2007) 1949–1966.
[95] D.V. Bavykin, J.M. Friedrich, F.C. Walsh, Adv. Mater. 18 (2006) 2807–2824.
[96] T. Maiyalagan, B. Viswanathan, U.V. Varadaraju, J. Nanosci. Nanotechnol. 6 (2006) 2067–2071.
[97] D. He, L. Yang, S. Kuang, Q. Cai, Electrochem. Commun. 9 (2007) 2467–2472.
[98] T. Okanishi, T. Matsui, T. Takeguchi, R. Kikuchi, K. Eguchi, Appl. Catal. A 298 (2006) 181–187.
[99] Z. Liu, B. Guo, L. Hong, T.H. Lim, Electrochem. Commun. 8 (2006) 83–90.
[100] E.E. Kohnke, J. Phys. Chem. Solids 23 (1962) 1557–1562.
[101] K.-S. Lee, I.-S. Park, Y.-H. Cho, D.-S. Jung, N. Jung, H.-Y. Park, Y.-E. Sung, J. Catal. 258 (2008) 143–152.
[102] H.L. Pang, X.H. Zhang, X.X. Zhong, B. Liu, X.G. Wei, Y.F. Kuang, J.H. Chen, J. Colloid Interface Sci. 319 (2008) 193–198.
[103] H.L. Pang, J.P. Lu, J.H. Chen, C.T. Huang, B. Liu, X.H. Zhang, Electrochim. Acta 54 (2009) 2610–2615.
[104] R.S. Hsu, D. Higgins, Z. Chen, Nanotechnology 21 (2010) 165705.
[105] C. Du, M. Chen, X. Cao, G. Yin, P. Shi, Electrochem. Commun. 11 (2009) 496–498.
[106] M.-W. Xu, G.-Y. Gao, W.-J. Zhou, K.-F. Zhang, H.-L. Li, J. Power Sources 175 (2008) 217–220.
[107] G.-Y. Zhao, H.-L. Li, Appl. Surf. Sci. 254 (2008) 3232–3235.
[108] C. Zhou, H. Wang, F. Peng, J. Liang, H. Yu, J. Yang, Langmuir 25 (2009) 7711–7717.
[109] L. Li, Z.-F. Yan, Studies Surf. Sci. Catal. 156 (2005) 523–528.
[110] R. Liu, S.B. Lee, J. Am. Chem. Soc. 130 (2008) 2942–2943.
[111] A.H. Gemeay, R.G. El-Sharkawy, I.A. Mansour, A.B. Zaki, Appl. Catal. B 80 (2008) 106–115.
[112] J. Li, L. Cui, X. Zhang, Appl. Surf. Sci. 256 (2010) 4339–4343.
[113] A.V. Murugan, C.W. Kwon, G. Campet, B.B. Kale, A.B. Mandale, S.R. Sainker, C.S. Gopinath, K. Vijayamohanan, J. Phys. Chem. B 108 (2004) 10736–10742.
[114] M. Malta, R.M. Torresi, Electrochim. Acta 50 (2005) 5009–5014.
[115] K.-I. Park, H.-M. Song, Y. Kim, S.-I. Mho, W.I. Cho, I.-H. Yeo, Electrochim. Acta, in press.
[116] B. Rajesh, K.R. Thampi, J.-M. Bonard, N. Xanthapolous, H.J. Mathieu, B. Viswanathan, Electrochem. Solid-State Lett. 5 (2002) E71–E74.
[117] T. Maiyalagan, B. Viswanathan, Mater. Chem. Phys. 121 (2010) 165–171.
[118] H. Pang, C. Huang, J. Chen, B. Liu, Y. Kuang, X. Zhang, J. Solid State Electrochem. 14 (2010) 169–174.